Investigation of the $D_s^+ \to K^+\pi^+\pi^-$ decay

Wei Liang,[1] Jing-Yu Yi,[2] C. W. Xiao,[3,1,*] and S. Q. Zhou[1]
[1]School of Physics, Central South University, Changsha 410083, China
[2]School of Physics and Electronics, Hunan University, 410082 Changsha, China
[3]Department of Physics, Guangxi Normal University, Guilin 541004, China

(Received 1 September 2023; accepted 7 November 2023; published 4 December 2023)

In the present work, we investigate the decay $D_s^+ \to K^+\pi^+\pi^-$ theoretically via considering the final state interaction formalism, where the W-external and -internal emission mechanisms in the hadronization processes of quark level are taken into account. In the hadron level, not only does the S-wave scattering amplitude contribute to the invariant mass distributions, but the contributions from the resonances $K^*(892)$, $K^*(1430)$, ρ, $\rho(1450)$, and $f_0(1370)$ are also considered. For the combined fit of the $\pi^+\pi^-$, $K^+\pi^+$, and $K^+\pi^-$ invariant mass spectra measured by the BESIII Collaboration, we take the coherent effects between the S and P waves into account and obtain consistent results with the experimental measurements. Moreover, we also calculate the branching fractions for each decay channel, some of which are in good agreement with the experiments.

DOI: 10.1103/PhysRevD.108.116001

I. INTRODUCTION

The hadronic decays of the D_s meson, which contains the charm and strangeness quarks, can be tested with the nonperturbative properties of quantum chromodynamics (QCD), which have caught much attention both in theories and experiments. Thus, in recent years the investigation for these decays has made great progress both experimentally and theoretically. In particular, in experiments, the CLEO, Belle, *BABAR*, and BESIII Collaborations, and so on, have studied nonleptonic three-body decay of D_s families with Dalitz plot analysis and measured the related branching fractions of intermediate resonances [1]. Some recent progress can be found in Ref. [2].

The E678 Collaboration once analyzed the $D_s^+(D^+) \to K^+K^-\pi^+$ decay with the Dalitz plot analyses and obtained the decay fractions and relative phases for different intermediate states [3], such as $\bar{K}^*(892)^0$, ϕ, $f_0(980)$, and so on, which were confirmed later by the measurements of the CLEO [4] and *BABAR* [5] Collaborations. Meanwhile, in Ref. [5] the relative branching fraction of the decay $D_s^+(D^+) \to K^+K^-\pi^+$ and the other two decays $D_s^+ \to K^+K^+\pi^-$ and $K^+K^+K^-$ were also measured through a Dalitz plot analysis. The branching fractions for the $D_s^+(D^+) \to K^+K^-\pi^+$ decay were reported by the CLEO [6] and *BABAR* [7] Collaborations, given by $(5.50 \pm 0.23 \pm 0.16)\%$ and $(5.78 \pm 0.20 \pm 0.30)\%$, respectively. Subsequently, an improved measurement of the branching fractions for the $D_s^+ \to K^+K^-\pi^+$ decay were done by the Belle [8] and CLEO [9] Collaborations, obtained as $(5.06 \pm 0.15 \pm 0.21)\%$ and $(5.55 \pm 0.14 \pm 0.13)\%$, respectively, which were consistent with the recent result of the BESIII Collaboration, $(5.47 \pm 0.08 \pm 0.13)\%$ [10]. The ratio of the branching fractions $B(D_s^+ \to \pi^+\pi^-\pi^+)/B(D_s^+ \to K^+K^-\pi^+)$ was measured by the *BABAR* Collaboration with a high precision [11]. Recently, the BESIII Collaboration reported the results for the $D_s^+ \to \pi^+\pi^-\pi^+$ decay [12], which were consistent with the latest measurements of the LHCb Collaboration [13], and where the contributions from the S wave $\pi^+\pi^-$ were found to be dominant and the contributions from the P and D waves, such as the intermediate states $\rho(770)$ and $f_2(1270)$, were also considered. Reference [13] also considered the contributions from the $\omega(782)$, $\rho(1700)$, and $f_2'(1525)$ resonances and compared the resonant contributions with the $D^+ \to \pi^+\pi^-\pi^+$ decay to indicate the dominant mechanisms of the tree-level W emission and the final state rescattering in the decay procedure. Analogously, using the first amplitude analysis to the decay $D_s^+ \to \pi^+\pi^0\eta$, its branching fraction was measured with significantly improved precision in Ref. [14], which claimed that the dominant W-annihilation decays $D_s^+ \to a_0(980)^+\pi^0$ and $D_s^+ \to a_0(980)^0\pi^+$ were observed for the first time and the related absolute branching fractions were found to be larger than the other measured pure W-annihilation decays. The branching fraction of the decay $D_s^+ \to K_S^0K_S^0\pi^+$ was measured by the BESIII Collaboration in Ref. [15], where the contributions from the resonances $S(1710)$, the ones $f_0(1710)$ and $a_0(1710)$, were determined. An enhancement in the $K_S^0K_S^0$ invariant mass spectrum near 1.7 GeV/c^2 was found [15], which implied the existence of the resonance

*xiaochw@gxnu.edu.cn

 © 2023 American Physical Society

$a_0(1710)$. Note that this enhancement was not seen in the decay $D_s^+ \to K^+K^-\pi^+$ [10]. A precise measurement of the absolute branching fraction $B(D_s^+ \to K_S^0K^+\pi^0)$ was done in Ref. [16], where an a_0-like state around 1817 MeV was found in the $K_S^0K^+$ invariant mass spectrum and this state was assumed as the isovector partner of the $f_0(1710)$ state at first. Recently, the BESIII Collaboration reported the amplitude analysis results for the $D_s^+ \to K^+\pi^+\pi^-$ decay [17], which had been measured in an early work of the FOCUS Collaboration [18], and was found that, except for the main contributions from the resonances ρ and $K^*(892)$, the contributions from the intermediate states $f_0(500)$, $f_0(980)$, and $f_0(1370)$ in this decay process were observed for the first time.

Furthermore, these experimental findings have drawn much theoretical attention, which provided an opportunity to investigate the production and properties of the resonances that appeared in these decay processes [19]. The decay properties of the D_s meson were studied in Ref. [20] using a four-flavor extended linear σ model, where the obtained weak decay constants were in good agreement with the experimental results. Motivated by the measurements reported by the BESIII Collaboration [10], the K^+K^- invariant mass distribution of the decay $D_s^+ \to K^+K^-\pi^+$ was investigated in Ref. [21] with the final state interaction formalism under the chiral unitary approach (ChUA) [22–27], where the experimental data from the *BABAR* [5] and BESIII [10] Collaborations were analyzed to hint at the resonance contributions of $f_0(980)$ and $a_0(980)$. In fact, the decay $D_s^+ \to K^+K^-\pi^+$ combined with $D_s^+ \to \pi^+\pi^-\pi^+$ were earlier studied in Ref. [28] with a similar approach, and the invariant mass distributions of the K^+K^- and $\pi^+\pi^-$ pairs were consistent with the experimental data [5,11] with a clear signal of the $f_0(980)$ state. Furthermore, a full analysis of the K^+K^-, $K^\pm\pi^+$ invariant mass spectra for the decay $D_s^+ \to K^+K^-\pi^+$ was performed in Ref. [29] by considering the resonance contributions from both the S and P waves, where the experimental data were described well and the obtained corresponding branching fractions were in agreement with the measurements of the BESIII Collaboration [10] and Particle Data Group (PDG) [30]. In addition, two decays $D_s^+ \to K^+K^+\pi^-$ and $D^+ \to K^-\pi^+\pi^+$ were investigated by using a naive factorization approach in Ref. [31] based on the analysis of the semileptonic decays $D^+ \to K^-\pi^+\ell^+\nu_\ell(\ell = e, \mu)$. Using a Khuri-Treiman formalism under the dispersion theory, the $D^+ \to K^-\pi^+\pi^+$ decay was analyzed in detail in Refs. [32,33], where the experimental data were described well by considering the contribution from the higher partial waves. Reference [34] adopted the W-internal emission mechanism to describe the $D_s^+ \to \pi^+\pi^0\eta$ decay with the contribution from the $a_0(980)$ resonance, which was dynamically generated from the coupled channel interactions of $K\bar{K}$ and $\pi\eta$; they solved the puzzle of the measured absolute branching fractions larger than those of other measured pure W-annihilation decays found in Ref. [14]. Moreover, the large branching fractions for the $D_s^+ \to \pi^+\pi^0\eta$ decay [14] were also explained in Ref. [35] with the triangle rescattering mechanism of $\rho\pi\eta^{(\prime)}$. More concerns on the $D_s^+ \to \pi^+\pi^0\eta$ decay can be found in [36,37]. With a phenomenological model, the production of the scalar resonances $f_0(500)$ and $f_0(980)$ was discussed in detail for the decay $D_{(s)}^+ \to \pi^+\pi^-\pi^+$ in Ref. [38], where some theoretical predictions for the decay $D_{(s)}^+ \to \pi^+\pi^0\pi^0$ were also made. In fact, the decay $D_s^+ \to \pi^+\pi^0\pi^0$ had been measured by the BESIII Collaboration [39], of which the results were investigated in Refs. [40–42] with the resonance contribution in the final state interactions. With the final state interaction formalism under the ChUA, Ref. [43] analyzed the $D_s^+ \to K_S^0K_S^0\pi^+$ decay to understand the properties of $a_0(1710)$, the isovector partner of $f_0(1710)$, and obtained good reproduction of the experimental data for the $K_S^0K_S^0$ and $K_S^0\pi^+$ invariant mass distributions [15]. Moreover, the experimental results of the $D_s^+ \to K_S^0K_S^0\pi^+$ decay [15] were also studied in a further work [44] to reveal the nature of the states $f_0(1710)$ and $a_0(1710)$, where the prediction for the branching ratio of $a_0(1710)$ in the $D_s^+ \to K_S^0K^+\pi^0$ decay was made, obtained as $\mathrm{Br}(D_s^+ \to \pi^0a_0(1710), a_0(1710) \to K^+K_S^0) = (1.3 \pm 0.4) \times 10^{-3}$. After the experimental finding [16], Ref. [45] investigated the $D_s^+ \to K_S^0K^+\pi^0$ reaction by considering the resonance contribution from $a_0(980)$ and $a_0(1710)$ in the final state interactions and reproduced the experimental invariant mass distributions well. To investigate the nature of the resonances $a_0(980)$ and $a_0(1710)$, a former work by two of the current authors [46] also concerned the productions of these resonances in the $D_s^+ \to K_S^0K^+\pi^0$ decay and made a full analysis for the invariant mass distributions of $K_S^0K^+$, $K^+\pi^0$, and $K_S^0\pi^0$ with a combined fit of the experimental data [16]. Furthermore, the evidence of the four-quark nature for the $f_0(500)$ and $f_0(980)$ states was discussed in detail in Ref. [47] based on the high-statistics experimental data from the BESIII Collaboration [48]. In the present work, motivated by the results of the $D_s^+ \to K^+\pi^+\pi^-$ decay measured by the BESIII Collaboration [17], we focus on this decay process with the final state interaction formalism to hint at the nature of the resonances $f_0(500)$ and $f_0(980)$. Note that, even though this singly Cabibbo-suppressed decay $D_s^+ \to K^+\pi^+\pi^-$ was measured in detail for the first time by the FOCUS Collaboration nearly 20 years ago [18], of which the branching fractions had been reported by the CLEO Collaboration [9], there is no theoretical work to investigate this decay (except for the one mentioned in the note added later).

Our work is organized as follows. In the next section, we introduce the formalism of final state interaction under the ChUA for the $D_s^+ \to K^+\pi^+\pi^-$ decay. In Sec. III, we show the main results, including the combined fitting results of

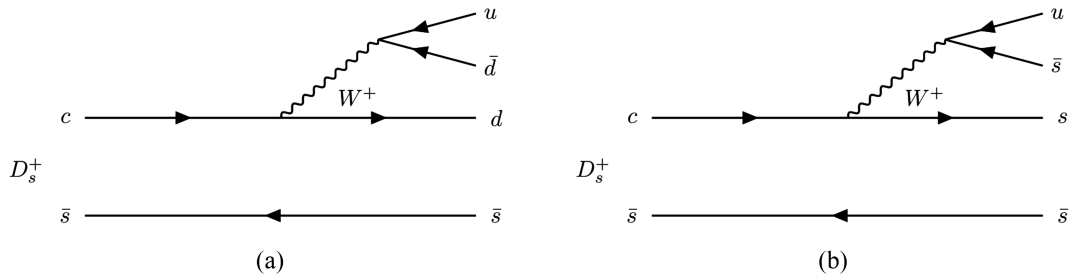

FIG. 1. W-external emission mechanism for the $D_s^+ \to K^+\pi^+\pi^-$ decay. (a) The creations of $u\bar{d}$ and $d\bar{s}$ quarks, (b) the creations of $u\bar{s}$ and $s\bar{s}$ quarks.

the experimental data for the $\pi^+\pi^-$, $K^+\pi^+$, and $K^+\pi^-$ invariant mass distributions, as well as the branching ratios of each decay process with different intermediate resonances. Finally, a short summary is displayed in Sec. IV.

II. FORMALISM

In the present work, we investigate the weak decay process of $D_s^+ \to K^+\pi^+\pi^-$ by considering the final state interactions under the coupled channel interaction formalism. As discussed in Refs. [19,34,49–51], the contributions of the weak decay topography can be divided into the following categories: W-external emission, W-internal emission, W-exchange and annihilation, and horizontal and vertical W loops, which have been ordered by their importance. Except for the first two types, the contribution from the others is extremely small due to the suppression of the helicity conservation and color factor. Therefore, we only consider the first two dominant diagrams, which are shown in Figs. 1 and 2, and omit the others. For the weak decay processes of the D_s^+ meson, as shown in Figs. 1 and 2, the component of the c quark can decay into a d or s quark by emitting a W^+ boson, which can further decay into a quark pair $u\bar{d}$ or $u\bar{s}$, and the component of the $\bar{s}$ quark can remain unchanged as a spectator.

For the case of the W-external emission as shown in Fig. 1, the quark pair $u\bar{d}$ ($u\bar{s}$) created by the W^+ boson forms a π^+ (K^+) meson directly, and the other quark pair $d\bar{s}$ ($s\bar{s}$) becomes two final states via the hadronization with quark pairs $q\bar{q} = u\bar{u} + d\bar{d} + s\bar{s}$ produced from the vacuum. Meanwhile, another situation also exists, where the quark pair $d\bar{s}$ ($s\bar{s}$) goes into a K^0 (η) and the other quark pair $u\bar{d}$ ($u\bar{s}$) made by the W^+ boson undergoes the hadronization. Thus, the corresponding decay procedures for these hadronizations can be written as

$$\begin{aligned} H^{(1a)} &= V_P V_{cd} V_{ud}\{(u\bar{d} \to \pi^+)[d\bar{s} \to d\bar{s}\cdot(u\bar{u} + d\bar{d} + s\bar{s})] \\ &\quad +(d\bar{s} \to K^0)[u\bar{d} \to u\bar{d}\cdot(u\bar{u} + d\bar{d} + s\bar{s})]\} \\ &= V_P V_{cd} V_{ud}\{(u\bar{d} \to \pi^+)[M_{23} \to (M\cdot M)_{23}] \\ &\quad +(d\bar{s} \to K^0)[M_{12} \to (M\cdot M)_{12}]\}, \end{aligned} \tag{1}$$

$$\begin{aligned} H^{(1b)} &= V'_P V_{cs} V_{us}\left\{(u\bar{s} \to K^+)[\bar{s}\,\bar{s} \to \bar{s}\,\bar{s}\cdot(u\bar{u} + d\bar{d} + s\bar{s})]\right. \\ &\quad \left.+\left(\bar{s}\,\bar{s} \to -\frac{2}{\sqrt{6}}\eta\right)[u\bar{s} \to u\bar{s}\cdot(u\bar{u} + d\bar{d} + s\bar{s})]\right\} \\ &= V'_P V_{cs} V_{us}\left\{(u\bar{s} \to K^+)[M_{33} \to (M\cdot M)_{33}]\right. \\ &\quad \left.+\left(\bar{s}\,\bar{s} \to -\frac{2}{\sqrt{6}}\eta\right)[M_{13} \to (M\cdot M)_{13}]\right\}. \end{aligned} \tag{2}$$

Similarly, for the other case of the W-internal emission, see Fig. 2, it also has two different hadronization processes. First, the pair $d\bar{d}$ ($s\bar{s}$) becomes the final state π^0 (η), and the other pair $u\bar{s}$ hadronizes into two hadrons with extra $q\bar{q}$ from the vacuum. Second, the pair $u\bar{s}$ goes into the K^+ directly, and the other pair $d\bar{d}$ ($s\bar{s}$) hadronizes into two final states with the $q\bar{q}$ pairs produced from the vacuum. Thus, these mechanisms can be expressed as

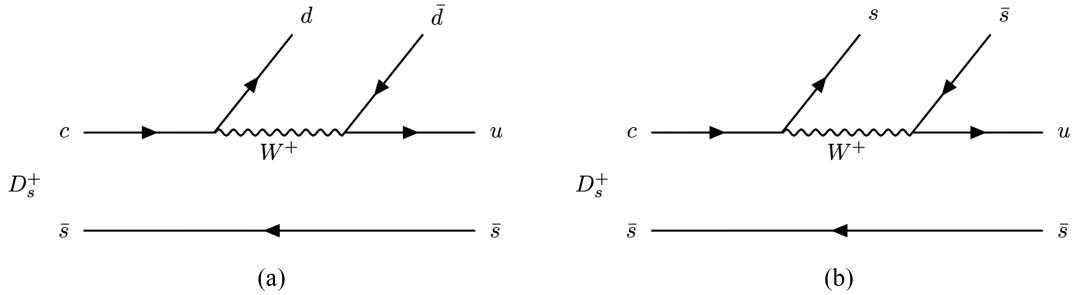

FIG. 2. W-internal emission mechanism for the $D_s^+ \to K^+\pi^+\pi^-$ decay. (a) The creations of $d\bar{d}$ and $u\bar{s}$ quarks, (b) the creations of $s\bar{s}$ and $u\bar{s}$ quarks.

$$H^{(2a)} = \beta V_P V_{cd} V_{ud}\Big\{\Big(d\bar{d}\to -\frac{1}{\sqrt{2}}\pi^0\Big)[u\bar{s}\to u\bar{s}\cdot(u\bar{u}+d\bar{d}+s\bar{s})]+\Big(d\bar{d}\to\frac{1}{\sqrt{6}}\eta\Big)[u\bar{s}\to u\bar{s}\cdot(u\bar{u}+d\bar{d}+s\bar{s})]$$
$$+(u\bar{s}\to K^+)[d\bar{d}\to d\bar{d}\cdot(u\bar{u}+d\bar{d}+s\bar{s})]\Big\}$$
$$=\beta V_P V_{cd} V_{ud}\Big\{\Big(d\bar{d}\to -\frac{1}{\sqrt{2}}\pi^0\Big)[M_{13}\to(M\cdot M)_{13}]+\Big(d\bar{d}\to\frac{1}{\sqrt{6}}\eta\Big)[M_{13}\to(M\cdot M)_{13}]$$
$$+(u\bar{s}\to K^+)[M_{22}\to(M\cdot M)_{22}]\Big\}, \tag{3}$$

$$H^{(2b)} = \beta V'_P V_{cs} V_{us}\Big\{\Big(s\bar{s}\to -\frac{2}{\sqrt{6}}\eta\Big)[u\bar{s}\to u\bar{s}\cdot(u\bar{u}+d\bar{d}+s\bar{s})]+(u\bar{s}\to K^+)[s\bar{s}\to s\bar{s}\cdot(u\bar{u}+d\bar{d}+s\bar{s})]\Big\}$$
$$=\beta V'_P V_{cs} V_{us}\Big\{\Big(s\bar{s}\to -\frac{2}{\sqrt{6}}\eta\Big)[M_{13}\to(M\cdot M)_{13}]+(u\bar{s}\to K^+)[M_{33}\to(M\cdot M)_{33}]\Big\}, \tag{4}$$

where the V_P and V'_P are the production vertex factors of the weak decay process, which can be assumed as constants [29,52,53] and determined by fitting the experimental data, see the results later. β is the coefficient, which presents the relative weight between the W-internal and W-external emission mechanisms [41,54]. The factors $-1/\sqrt{2}$, $1/\sqrt{6}$, and $-2/\sqrt{6}$ are due to the flavor components of the π^0 and η mesons, given by

$$|\pi^0\rangle = \frac{1}{\sqrt{2}}|(u\bar{u}-d\bar{d})\rangle, \qquad |\eta\rangle = \frac{1}{\sqrt{6}}|(u\bar{u}+d\bar{d}-2s\bar{s})\rangle. \tag{5}$$

The $V_{q_1q_2}$ is the element of the Cabibbo-Kobayashi-Maskawa (CKM) matrix for the quark transition $q_1\to q_2$, and the matrix M with $q\bar{q}$ elements in quark level of SU(3) is given by

$$M = \begin{pmatrix} u\bar{u} & u\bar{d} & u\bar{s} \\ d\bar{u} & d\bar{d} & d\bar{s} \\ s\bar{u} & s\bar{d} & s\bar{s} \end{pmatrix}. \tag{6}$$

After the hadronization, the SU(3) matrix M is transferred to the hadron level form in terms of the pseudoscalar meson fields, rewritten as

$$M\to\begin{pmatrix} \frac{1}{\sqrt{2}}\pi^0+\frac{1}{\sqrt{6}}\eta & \pi^+ & K^+ \\ \pi^- & -\frac{1}{\sqrt{2}}\pi^0+\frac{1}{\sqrt{6}}\eta & K^0 \\ K^- & \bar{K}^0 & -\frac{2}{\sqrt{6}}\eta \end{pmatrix}, \tag{7}$$

where we take $\eta\equiv\eta_8$ and do not consider the η_1 since it is not relevant to our present case, as done in Ref. [55]. In fact, the singlet of SU(3) components η_1 is always not considered in chiral perturbation theory [56], due to no interaction with it, see more discussions in Ref. [57]. Furthermore, we also do not taken into account the η-η' mixing for the threshold of the $\eta'\eta'$ channel far away from the energy region of our concern, where the resonance $f_0(980)$ appears in the S-wave coupled channel interactions. As found in Ref. [55], the contribution of η-η' mixing is small and has less effect on the final results, and thus, we ignore its contribution. More discussions on η-η' mixing in the SU(3) chiral effective field theory can be found in Ref. [58]. Then, the hadronization processes at the quark level in Eqs. (1)–(4) can be expressed in the hadron level as

$$(M\cdot M)_{12} = \frac{2}{\sqrt{6}}\pi^+\eta + K^+\bar{K}^0,$$
$$(M\cdot M)_{13} = \frac{1}{\sqrt{2}}\pi^0K^+ + \pi^+K^0 - \frac{1}{\sqrt{6}}\eta K^+,$$
$$(M\cdot M)_{22} = \pi^+\pi^- + \frac{1}{2}\pi^0\pi^0 + \frac{1}{6}\eta\eta - \frac{1}{\sqrt{3}}\pi^0\eta + K^0\bar{K}^0,$$
$$(M\cdot M)_{23} = \pi^-K^+ - \frac{1}{\sqrt{2}}\pi^0K^0 - \frac{1}{\sqrt{6}}K^0\eta,$$
$$(M\cdot M)_{33} = K^+K^- + K^0\bar{K}^0 + \frac{2}{3}\eta\eta. \tag{8}$$

Then, from Eqs. (1)–(4), we can get all the final states with π^+ (π^0), η, and K^+ (K^0) directly produced in the hadronization processes,

$$H^{(1a)} = V_P V_{cd} V_{ud}\Big(\pi^+\pi^-K^+ - \frac{1}{\sqrt{2}}\pi^+\pi^0K^0 + \frac{1}{\sqrt{6}}\pi^+K^0\eta + K^+K^0\bar{K}^0\Big), \tag{9}$$

$$H^{(1b)} = V'_P V_{cs} V_{us}\Big(K^+K^+K^- + K^+K^0\bar{K}^0 + K^+\eta\eta - \frac{1}{\sqrt{3}}\pi^0K^+\eta - \frac{2}{\sqrt{6}}\pi^+K^0\eta\Big), \tag{10}$$

$$H^{(2a)} = \beta \times V_P V_{cd} V_{ud}\left(\pi^+\pi^- K^+ + K^+ K^0 \bar{K}^0 - \frac{1}{\sqrt{2}}\pi^+\pi^0 K^0 + \frac{1}{\sqrt{6}}\eta\pi^+ K^0\right), \tag{11}$$

$$H^{(2b)} = \beta \times V'_P V_{cs} V_{us}\left(K^+ K^+ K^- + K^+ K^0 \bar{K}^0 + \eta\eta K^+ - \frac{1}{\sqrt{3}}\eta\pi^0 K^+ - \frac{2}{\sqrt{6}}\eta\pi^+ K^0\right). \tag{12}$$

Note that the elements of the CKM matrix have the following relationship, $V_{cd}V_{ud} = -V_{cs}V_{us}$ [30]. Thus, we can obtain the total contributions of the weak decay processes as shown in Figs. 1 and 2 for the decay $D_s^+ \to K^+\pi^+\pi^-$, having

$$\begin{aligned} H &= H^{(1a)} + H^{(1b)} + H^{(2a)} + H^{(2b)} \\ &= V_{cd}V_{ud}(1+\beta)\left[V_P\left(\pi^+\pi^- K^+ - \frac{1}{\sqrt{2}}\pi^+\pi^0 K^0 + \frac{1}{\sqrt{6}}\eta\pi^+ K^0 + K^+ K^0 \bar{K}^0\right)\right. \\ &\quad \left. + V'_P\left(-K^+ K^+ K^- - \eta\eta K^+ + \frac{2}{\sqrt{6}}\eta\pi^+ K^0 - K^+ K^0 \bar{K}^0 + \frac{1}{\sqrt{3}}\eta\pi^0 K^+\right)\right]. \end{aligned} \tag{13}$$

Since the $\eta\pi^0$ has isospin $I = 1$, it cannot contribute to the final states $\pi^+\pi^- K^+$ upon the rescattering process. Therefore, we have the total contributions finally,

$$\begin{aligned} H &= V_{cd}V_{ud}(1+\beta)\left[V_P\left(\pi^+\pi^- K^+ - \frac{1}{\sqrt{2}}\pi^+\pi^0 K^0 + \frac{1}{\sqrt{6}}\eta\pi^+ K^0 + K^+ K^0 \bar{K}^0\right)\right. \\ &\quad \left. - V'_P\left(K^+ K^+ K^- + \eta\eta K^+ - \frac{2}{\sqrt{6}}\eta\pi^+ K^0 + K^+ K^0 \bar{K}^0\right)\right] \\ &= C_1\left(\pi^+\pi^- K^+ - \frac{1}{\sqrt{2}}\pi^+\pi^0 K^0 + \frac{1}{\sqrt{6}}\eta\pi^+ K^0 + K^+ K^0 \bar{K}^0\right) \\ &\quad - C_2\left(K^+ K^+ K^- + \eta\eta K^+ - \frac{2}{\sqrt{6}}\eta\pi^+ K^0 + K^+ K^0 \bar{K}^0\right), \end{aligned} \tag{14}$$

where the factors C_1 and C_2 are defined as $C_1 = V_P V_{cd} V_{ud}(1+\beta)$ and $C_2 = V'_P V_{cd} V_{ud}(1+\beta)$, which also include the normalization factors when we fit to the experimental data later.

From Eq. (14), we can see that, except for the term $K^+\pi^+\pi^-$, which directly contributes to the final states on the tree-level hadronization processes, the other terms should be proceeded through the rescattering procedures to the final states $K^+\pi^+\pi^-$, as shown in Fig. 3. Thus, the amplitudes for these processes of the $D_s^+ \to K^+\pi^+\pi^-$ decay in the S wave can be written as

$$\begin{aligned} t(s_{12}, s_{23}) = C_1 &\left[1 + G_{\pi^- K^+}(s_{23}) T_{\pi^- K^+ \to \pi^- K^+}(s_{23}) + G_{\pi^+\pi^-}(s_{12}) T_{\pi^+\pi^- \to \pi^+\pi^-}(s_{12})\right. \\ &- \frac{1}{\sqrt{2}} G_{\pi^0 K^0}(s_{23}) T_{\pi^0 K^0 \to \pi^- K^+}(s_{23}) + \frac{1}{\sqrt{6}} G_{\eta K^0}(s_{23}) T_{\eta K^0 \to \pi^- K^+}(s_{23}) \\ &\left. + G_{K^0 \bar{K}^0}(s_{12}) T_{K^0 \bar{K}^0 \to \pi^+\pi^-}(s_{12})\right] - C_2\left[G_{K^+ K^-}(s_{12}) T_{K^+ K^- \to \pi^+\pi^-}(s_{12})\right. \\ &\left. + G_{\eta\eta}(s_{12}) T_{\eta\eta \to \pi^+\pi^-}(s_{12}) - \frac{2}{\sqrt{6}} G_{\eta K^0}(s_{23}) T_{\eta K^0 \to \pi^- K^+}(s_{23}) + G_{K^0 \bar{K}^0}(s_{12}) T_{K^0 \bar{K}^0 \to \pi^+\pi^-}(s_{12})\right], \end{aligned} \tag{15}$$

where $s_{ij} = (p_i + p_j)^2$ is the energy of the two-body system, p_i and p_j are the four-momenta of the corresponding particles, with the indices $i, j = 1, 2, 3$ representing three final states π^+, π^-, and K^+, respectively. It should be mentioned that there is a factor of 2 in the term related to the identical particles $\eta\eta$ in Eq. (15), which has been canceled with the $1/2$ factor in their propagators within our normalization scheme; more discussions are found in Ref. [59]. Furthermore, $G_{PP'}(s)$ is the loop function of two intermediate meson propagators, which can be written as

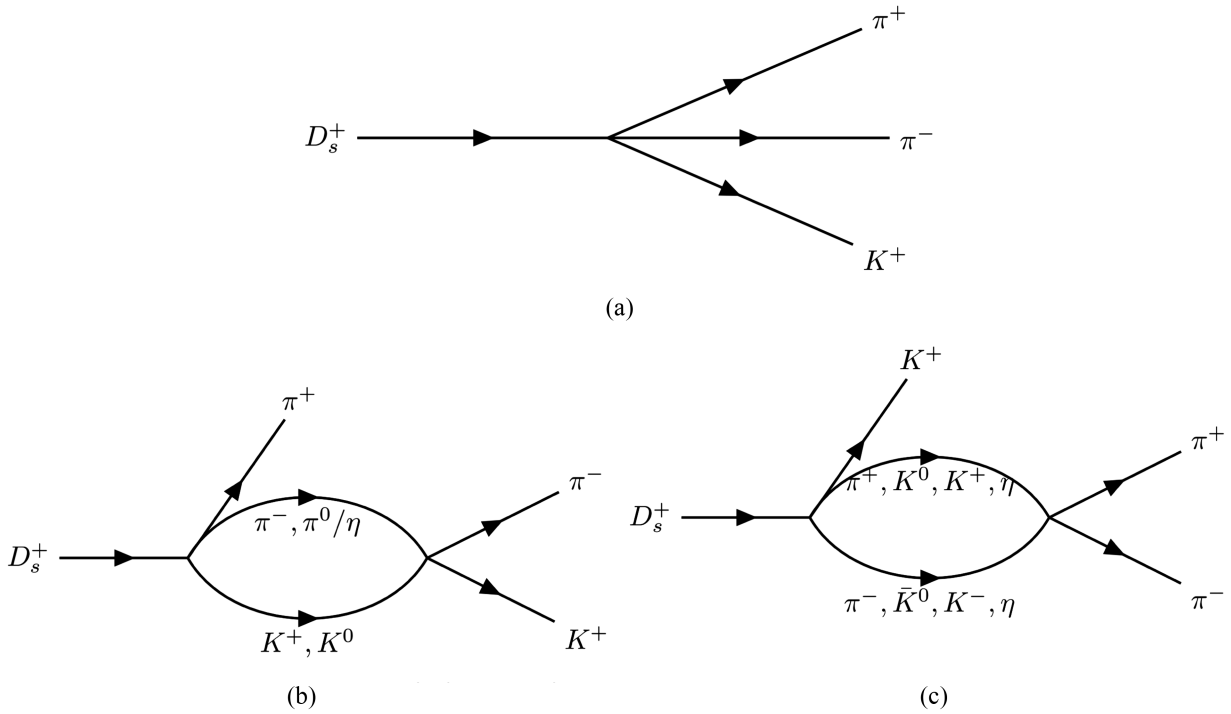

FIG. 3. Diagrammatic representations of the $D_s^+ \to K^+\pi^+\pi^-$ decay. (a) Tree-level production. (b) Rescattering of $K^+\pi^-$, $K^0\pi^0$, and $K^0\eta$. (c) Rescattering of $\pi^+\pi^-$, $K^0\bar{K}^0$, K^+K^-, and $\eta\eta$.

$$G_{PP'}(s) = i\int \frac{d^4q}{(2\pi)^4}\frac{1}{q^2 - m_1^2 + i\varepsilon}\frac{1}{(p_1+p_2-q)^2 - m_2^2 + i\varepsilon}, \tag{16}$$

where p_k are the four-momenta of the initial particles, m_k are the masses of the intermediate particles (P and P'), and $s = (p_1+p_2)^2$. Since the loop integral is logarithmically divergent, there are two ways to solve this singular integral. The first one is the three-momentum cutoff method [22,23,25,60], having

$$G_{PP'}(s) = \int_0^{q_{\max}} \frac{q^2 dq}{(2\pi)^2}\frac{\omega_1+\omega_2}{\omega_1\omega_2\left[s-(\omega_1+\omega_2)^2+i\varepsilon\right]}, \tag{17}$$

with $\omega_k = (\vec{q}^2 + m_k^2)^{1/2}$. The other one is the dimensional regularization method, of which the explicit form is given by [26,61–64]

$$\begin{aligned} G_{PP'}(s) = \frac{1}{16\pi^2}\Bigg\{ & a_\mu(\mu) + \ln\frac{m_1^2}{\mu^2} + \frac{m_2^2-m_1^2+s}{2s}\ln\frac{m_2^2}{m_1^2} \\ & + \frac{q_{cm}(s)}{\sqrt{s}}\left[\ln\left(s-(m_2^2-m_1^2)+2q_{cm}(s)\sqrt{s}\right)\right. \\ & + \ln\left(s+(m_2^2-m_1^2)+2q_{cm}(s)\sqrt{s}\right) \\ & - \ln\left(-s-(m_2^2-m_1^2)+2q_{cm}(s)\sqrt{s}\right) \\ & \left. - \ln\left(-s+(m_2^2-m_1^2)+2q_{cm}(s)\sqrt{s}\right)\right]\Bigg\}, \end{aligned} \tag{18}$$

where a_μ is the subtraction constant, of which the values for different channels will be introduced later, μ is the regularization scale, which is chosen as 0.6 GeV with the value of cutoff $q_{\max}$ from Refs. [22,28,36,57], and $q_{cm}(s)$ is the three-momentum of the particle in the center-of-mass frame, given by

$$q_{cm}(s) = \frac{\lambda^{1/2}(s, m_1^2, m_2^2)}{2\sqrt{s}}, \tag{19}$$

with the Källén triangle function $\lambda(a,b,c) = a^2+b^2+c^2-2(ab+ac+bc)$. Note that the parameters a_μ and μ are not independent of each other [see the first two terms of Eq. (18)], between which the relationship can be found in Refs. [26,65] and on which more discussions can be found in Refs. [66–68]. In our work, we adopt the latter method for our main calculations, where, of course, the choice of these two regularization methods does not affect our conclusions. Additionally, $T_{P_mP_n\to P_{m'}P_{n'}}$ in Eq. (15) is the two-body scattering amplitude, which can be calculated by the coupled channel Bethe-Salpeter equation of the ChUA [22,23],

$$T = [1 - VG]^{-1}V. \tag{20}$$

Note that the matrix G is constructed by the loop functions, which is a diagonal matrix with the elements given by Eq. (16), and the matrix V is made of the interaction potentials for each coupled channel, which can

be evaluated from the chiral Lagrangians. In the present work, for the $I = 0$ sector, there are five coupled channels, $\pi^+\pi^-(1)$, $\pi^0\pi^0(2)$, $K^+K^-(3)$, $K^0\bar{K}^0(4)$, and $\eta\eta(5)$, and thus, the elements of the 5×5 symmetric V matrix are given by [29,52,57]

$$
\begin{aligned}
V_{11} &= -\frac{1}{2f^2}s, \qquad V_{12} = -\frac{1}{\sqrt{2}f^2}(s-m_\pi^2), \qquad V_{13} = -\frac{1}{4f^2}s,\\
V_{14} &= -\frac{1}{4f^2}s, \qquad V_{15} = -\frac{1}{3\sqrt{2}f^2}m_\pi^2, \qquad V_{22} = -\frac{1}{2f^2}m_\pi^2,\\
V_{23} &= -\frac{1}{4\sqrt{2}f^2}s, \qquad V_{24} = -\frac{1}{4\sqrt{2}f^2}s, \qquad V_{25} = -\frac{1}{6f^2}m_\pi^2,\\
V_{33} &= -\frac{1}{2f^2}s, \qquad V_{34} = -\frac{1}{4f^2}s,\\
V_{35} &= -\frac{1}{12\sqrt{2}f^2}(9s-6m_\eta^2-2m_\pi^2), \qquad V_{44} = -\frac{1}{2f^2}s,\\
V_{45} &= -\frac{1}{12\sqrt{2}f^2}(9s-6m_\eta^2-2m_\pi^2),\\
V_{55} &= -\frac{1}{18f^2}(16m_K^2-7m_\pi^2).
\end{aligned}
\tag{21}
$$

For the $I = 1/2$ sector, three channels are coupled, $K^+\pi^-(1)$, $K^0\pi^0(2)$, $K^0\eta(3)$, and then the elements of 3×3 symmetric matrix are given by [29]

$$
\begin{aligned}
V_{11} &= \frac{-1}{6f^2}\left[\frac{3}{2}s-\frac{3}{2s}(m_\pi^2-m_K^2)^2\right],\\
V_{12} &= \frac{1}{2\sqrt{2}f^2}\left[\frac{3}{2}s-m_\pi^2-m_K^2-\frac{(m_\pi^2-m_K^2)^2}{2s}\right],\\
V_{13} &= \frac{1}{2\sqrt{6}f^2}\left[\frac{3}{2}s-\frac{7}{6}m_\pi^2-\frac{1}{2}m_\eta^2-\frac{1}{3}m_K^2+\frac{3}{2s}(m_\pi^2-m_K^2)(m_\eta^2-m_K^2)\right],\\
V_{22} &= \frac{-1}{4f^2}\left[-\frac{s}{2}+m_\pi^2+m_K^2-\frac{(m_\pi^2-m_K^2)^2}{2s}\right],\\
V_{23} &= -\frac{1}{4\sqrt{3}f^2}\left[\frac{3}{2}s-\frac{7}{6}m_\pi^2-\frac{1}{2}m_\eta^2-\frac{1}{3}m_K^2+\frac{3}{2s}(m_\pi^2-m_K^2)(m_\eta^2-m_K^2)\right],\\
V_{33} &= -\frac{1}{4f^2}\left[-\frac{3}{2}s-\frac{2}{3}m_\pi^2+m_\eta^2+3m_K^2-\frac{3}{2s}(m_\eta^2-m_K^2)^2\right],
\end{aligned}
\tag{22}
$$

where $f = 0.093$ GeV is the pion decay constant [22], and m_P is the corresponding mass of pseudoscalar mesons. Note that the phase convention for the isospin basis is $|\pi^+\rangle = -|1,1\rangle$ and $|K^+\rangle = -|\frac{1}{2},\frac{1}{2}\rangle$ [22].

As we know, for the contribution of the W-external emission in Fig. 1, the quark pair $d\bar{s}$ not only can form $K^+\pi^-$ via hadronization in the S wave, but also can produce the intermediate states $K^*(892)^0/K_0^*(1430)^0$ in the P/S waves, which decays into the $K^+\pi^-$ final states. Similarly, for the W-internal emission of Fig. 2, the $d\bar{d}$ quark pair also can form $\rho/\rho(1450)$ and $f_0(1370)$ mesons in the P and S waves, respectively, and then decay into the $\pi^+\pi^-$ final states. These production mechanisms are depicted in Fig. 4. The full relativistic amplitude for these decays can be written as [55]

$$
\begin{aligned}
M_{K^*(892)}(s_{12},s_{23}) = &\frac{D_{K^*(892)}e^{i\alpha_{K^*(892)}}}{s_{23}-m_{K^*(892)}^2+im_{K^*(892)}\Gamma_{K^*(892)}}\\
&\times\left[(m_K^2-m_\pi^2)\frac{m_{D_s^+}^2-m_\pi^2}{m_{K^*(892)}^2}-s_{13}+s_{12}\right],
\end{aligned}
\tag{23}
$$

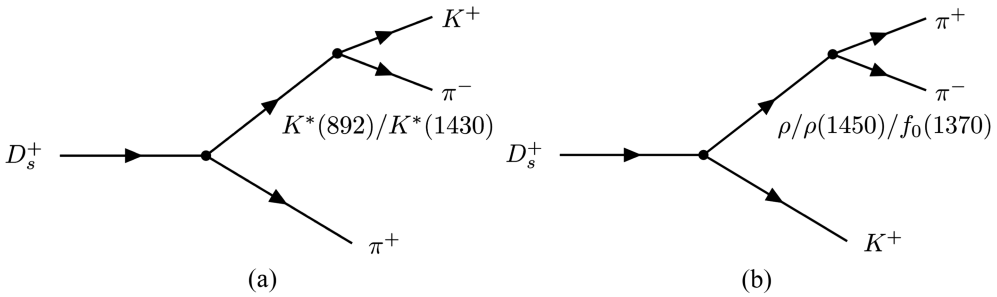

FIG. 4. Mechanisms for the $D_s^+ \to K^+\pi^+\pi^-$ decay process through intermediate states. (a) Diagram via $K^*(892)$, $K^*(1430)$. (b) Diagram via ρ, $\rho(1450)$, and $f_0(1370)$.

$$M_{K^*(1430)}(s_{12},s_{23}) = \frac{D_{K^*(1430)}e^{i\alpha_{K^*(1430)}}}{s_{23}-m^2_{K^*(1430)}+im_{K^*(1430)}\Gamma_{K^*(1430)}} \times [(s_{23}-m_K^2-m_\pi^2) \cdot (s_{13}+s_{12}-m_K^2-m_\pi^2)], \tag{24}$$

$$M_{f_0(1370)}(s_{12},s_{23}) = \frac{D_{f_0(1370)}e^{i\alpha_{f_0(1370)}}}{s_{12}-m^2_{f_0(1370)}+im_{f_0(1370)}\Gamma_{f_0(1370)}} \times [(s_{12}-2m_\pi^2)\cdot(s_{13}+s_{23}-2m_\pi^2)], \tag{25}$$

$$M_\rho(s_{12},s_{23}) = \frac{D_\rho e^{i\alpha_\rho}}{s_{12}-m_\rho^2+im_\rho\Gamma_\rho}(s_{23}-s_{13}), \tag{26}$$

where the $D_{K^*(892)/K^*(1430)/f_0(1370)/\rho}$ and $\alpha_{K^*(892)/K^*(1430)/f_0(1370)/\rho}$ are the normalization constants and the phases, respectively, which can be obtained by fitting the experimental data, see our results later. Additionally, the $\Gamma_{K^*(892)/K^*(1430)/f_0(1370)/\rho}$ and $m_{K^*(892)/K^*(1430)/f_0(1370)/\rho}$ are the total widths and masses of these intermediate states, respectively, of which the values are taken from the PDG [30]. By the way, the amplitude of $\rho(1450)$ is similar to the one of ρ, which can be obtained via changing the values of the corresponding width and mass and introducing two more free parameters, $D_{\rho(1450)}$ and $\alpha_{\rho(1450)}$. Note that the variables s_{ij} are not independent totally and fulfill the constraint condition,

$$s_{12}+s_{23}+s_{13} = m^2_{D_s^+}+m^2_{K^+}+m^2_{\pi^+}+m^2_{\pi^-}, \tag{27}$$

which indicates that only two of the s_{ij} are independent.

Finally, considering the coherence as done in Refs. [21,29,35,37,69], the double differential width distribution for the three-body decay $D_s^+ \to K^+\pi^+\pi^-$ can be calculated by [30]

$$\frac{d^2\Gamma}{ds_{12}ds_{23}} = \frac{1}{(2\pi)^3}\frac{1}{32m^3_{D_s^+}}\Big(|t(s_{12},s_{23}) + M_{K^*(892)} + M_{K^*(1430)} + M_{f_0(1370)} + M_\rho + M_{\rho(1450)}|^2\Big). \tag{28}$$

Thus, the invariant mass spectra $d\Gamma/ds_{12}$ and $d\Gamma/ds_{23}$ can be obtained by integrating the other invariant variables in Eq. (28). Meanwhile, $d\Gamma/ds_{13}$ can be obtained via Eq. (27). For the limits of integration, taken from the PDG [30], we have

$$(s_{23})_{\max} = (E_2^*+E_3^*)^2 - \left(\sqrt{E_2^{*2}-m_2^2}-\sqrt{E_3^{*2}-m_3^2}\right)^2, \tag{29}$$

$$(s_{23})_{\min} = (E_2^*+E_3^*)^2 - \left(\sqrt{E_2^{*2}-m_2^2}+\sqrt{E_3^{*2}-m_3^2}\right)^2, \tag{30}$$

where $E_2^* = (s_{12}-m_1^2+m_2^2)/2\sqrt{s_{12}}$ and $E_3^* = (m^2_{D_s^+}-s_{12}-m_3^2)/2\sqrt{s_{12}}$. As mentioned in Refs. [29,55,70], the ChUA has a limit on the effective energy range. Therefore, in order to make reliable calculation in the higher energy region, we should extrapolate the scattering amplitude above the energy cut $\sqrt{s_{\rm cut}} = 1.1$ GeV smoothly,[1]

$$G(s)T(s) = G(s_{\rm cut})T(s_{\rm cut})e^{-\alpha(\sqrt{s}-\sqrt{s_{\rm cut}})}, \quad \text{for } \sqrt{s} > \sqrt{s_{\rm cut}}, \tag{31}$$

where G is the loop function of two meson propagators as mentioned above, T is the scattering amplitude obtained by

[1]Note that only one parameter was used in Refs. [22,71] with the ChUA, where the experimental data were described well up to 1.2 GeV. Thus, the results of $K\bar{K}$ interactions with its coupled channels were still trustworthy for $\sqrt{s} < 1.2$ GeV as commented in Ref. [72]. In the present work, we are only interested in the resonance region of $f_0(980)$ below 1.1 GeV.

the coupled channel interactions above, and α is a smoothing extrapolation parameter, of which the value will be determined in the next section.

III. RESULTS

As mentioned in the previous section, we need to determine the subtraction constant a_μ for different decay channels in the loop functions. In fact, we can get these values by connecting two regularization methods, which means that the loop functions with different regularization methods at the threshold for certain channels have the same values. Then, for the given μ, a relationship between the free parameters a_μ and $q_{\max}$ is obtained as [60,71]

$$a_\mu = 16\pi^2[G^{CO}(s_{\rm thr}, q_{\max}) - G^{DR}(s_{\rm thr}, \mu)], \quad (32)$$

with G^{CO} and G^{DR} given by Eqs. (17) and (18), respectively, and taking $\mu = q_{\max} = 0.6$ GeV as mentioned above. For the $I = 0$ sector, we can get

$$a_{\pi^+\pi^-} = -1.30, \quad a_{\pi^0\pi^0} = -1.29, \quad a_{K^+K^-} = -1.63,$$
$$a_{K^0\bar{K}^0} = -1.63, \quad a_{\eta\eta} = -1.68. \quad (33)$$

Similarly, for the $I = 1/2$ sector, the subtraction constants are obtained as

$$a_{\pi^-K^+} = -1.57, \quad a_{\pi^0K^0} = -1.57, \quad a_{\eta K^0} = -1.66. \quad (34)$$

Therefore, the free parameters in our formalism are C_1, C_2, and α in the S wave and D_ρ, α_ρ, $D_{K^*(892)}$, $\alpha_{K^*(892)}$, $D_{f_0(1370)}$, $\alpha_{f_0(1370)}$, $D_{K^*(1430)}$, $\alpha_{K^*(1430)}$, $D_{\rho(1450)}$, and $\alpha_{\rho(1450)}$ for the S/P-wave resonance contributions, which can be determined by fitting the experimental data. As mentioned in the last section, the coherence between the S and P waves is taken into account. In fact, we have made a test with the incoherence for them and obtained similar results with a bit worse total χ^2. In order to describe the invariant mass distributions of $\pi^+\pi^-$, $K^+\pi^+$, and $K^+\pi^-$ simultaneously, we make a combined fit with the BESIII experimental data, where the fitted parameters are presented in Table I. Meanwhile, with these fitted parameters, we can get the contribution of intermediate resonances ρ, $K^*(892)$, $K^*(1430)$, $f_0(1370)$, and $\rho(1450)$ in different invariant mass distributions and show the best fitted results in Fig. 5.

In the $\pi^+\pi^-$ invariant mass distributions as shown in Fig. 5(a), one can clearly see that the structure around 0.8 GeV is the contribution of the ρ resonance, while the narrow peak at 0.98 GeV of our results represents the signal of the dynamical generation of the resonance $f_0(980)$. Note that the effect of the $f_0(980)$ in the $\pi^+\pi^-$ distribution of the $\bar{B}^0 \to \pi^+\pi^- D^0$ decay is also important [73], while this signal in experiment is not so visible [17]. Additionally, the wide bump structure around the low energy region is, in fact, the contributions from the resonances $f_0(500)$ and $K^*(892)$, whereas the one in the high energy region is mainly contributed from the states $K^*(892)$ and $f_0(1370)$, where the other resonances play little role in this spectrum. In Fig. 5(b), the $K^+\pi^+$ invariant mass distributions are presented, where one can find that the bumps in the low energy region benefits from the ρ resonance, which also contributes to the peak around 1.7 GeV. Meanwhile, the influence of the $K^*(892)$ state around 1.7 GeV is also important, which also dominates the region of 1.1–1.3 GeV. Finally, the $K^+\pi^-$ distributions are plotted in Fig. 5(c), where the first peak below 1.0 GeV is caused by the state $K^*(892)$, and the other two wide structures in the high energy region are dominated by the resonances $K_0^*(1430)$ and ρ, $\rho(1450)$, respectively. Moreover, the signals closed to the threshold and below the $K^*(892)$ peak are contributed from the states ρ, $\rho(1450)$ in the P wave and $f_0(500)$ in the S wave.

In addition, we also calculate the ratios of the branching fractions for different decay channels based on the fitting results. Since the unknown weak production vertex factors and normalization factors have been absorbed into the fitting parameters, to reduce the uncertainties, it is better to evaluate the ratios of the branching fractions for different channels due to the cancellation of these factors, which are more reliable. Thus, by integrating the $\pi^+\pi^-$ and $K^+\pi^-$ invariant mass distributions, we get results as follows:

$$\frac{\mathcal{B}[D_S^+ \to K^+ f_0(500) \to K^+\pi^+\pi^-]}{\mathcal{B}\left[D_S^+ \to K^*(892)^0\pi^+ \to K^+\pi^+\pi^-\right]} = 0.20^{+0.02}_{-0.02},$$
$$\frac{\mathcal{B}[D_S^+ \to K^+ f_0(980) \to K^+\pi^+\pi^-]}{\mathcal{B}\left[D_S^+ \to K^*(892)^0\pi^+ \to K^+\pi^+\pi^-\right]} = 0.06^{+0.02}_{-0.02},$$
$$\frac{\mathcal{B}[D_S^+ \to K^+\rho \to K^+\pi^+\pi^-]}{\mathcal{B}\left[D_S^+ \to K^*(892)^0\pi^+ \to K^+\pi^+\pi^-\right]} = 1.59^{+0.02}_{-0.03},$$
$$\frac{\mathcal{B}[D_S^+ \to f_0(1370)K^+ \to K^+\pi^+\pi^-]}{\mathcal{B}\left[D_S^+ \to K^*(892)^0\pi^+ \to K^+\pi^+\pi^-\right]} = 0.58^{+0.06}_{-0.11},$$
$$\frac{\mathcal{B}[D_S^+ \to K^+\rho(1450) \to K^+\pi^+\pi^-]}{\mathcal{B}\left[D_S^+ \to K^*(892)^0\pi^+ \to K^+\pi^+\pi^-\right]} = 1.28^{+0.02}_{-0.05},$$
$$\frac{\mathcal{B}[D_S^+ \to K^*(1430)\pi^- \to K^+\pi^+\pi^-]}{\mathcal{B}\left[D_S^+ \to K^*(892)^0\pi^+ \to K^+\pi^+\pi^-\right]} = 0.57^{+0.01}_{-0.01}, \quad (35)$$

where the integral limits of the central values for the $D_s^+ \to K^+ f_0(500)$, $K^+\rho$ processes are from the threshold to 0.9 and 1.1 GeV, respectively, and the uncertainties are due to the limits 0.9 ± 0.05 and 1.1 ± 0.05 GeV, respectively. For the $D_s^+ \to K^+ f_0(980)$ process, the central values of the integral limits are from 0.9 to 1.1 GeV, and the uncertainties come from 0.9 ± 0.05 and 1.1 ± 0.05 GeV, respectively. For the $D_s^+ \to f_0(1370)K^+$, $\rho(1450)K^+$ decays, the integral limits

TABLE I. Values of the parameters from the fit.

Parameters	C_1	C_2	α	D_ρ	α_ρ	$D_{K^*(892)}$	$\alpha_{K^*(892)}$
Fit	263.74	−63.08	12.34	80.77	0.18	62.99	3.54
Parameters	$D_{K^*(1430)}$	$\alpha_{K^*(1430)}$	$D_{f_0(1370)}$	$\alpha_{f_0(1370)}$	$D_{\rho(1450)}$	$\alpha_{\rho(1450)}$	χ^2/d.o.f.
Fit	−62.50	1.21	−60.24	3.07	−456.70	0.93	1.43

are taken from the threshold to 1.4 GeV, while the ones for the $D_s^+ \to K_0^*(1430)\pi^-$ decay are up to 1.7 GeV, and the uncertainties come from the changes of 1.4 ± 0.05 and 1.7 ± 0.05, respectively. Then, taking the branching fraction of the decay channel via $K^*(892)^0$ measured by the BESIII Collaboration $B[D_S^+ \to K^*(892)^0\pi^+, K^*(892)^0 \to K^+\pi^-] = (1.85 \pm 0.13 \pm 0.11) \times 10^{-3}$ [17] as input, we can calculate the branching fractions for the different intermediate process, where the results are presented in Table II. It is found that the branching of the intermediate states ρ and $\rho(1450)$ are obviously bigger than the experimental measurements due to the interference between the P-wave amplitudes, which can be seen from their line shape in Fig. 5(a), and the one for the contribution of the $f_0(980)$ is nearly one-half smaller than the measurements; whereas, the branching fractions of the other intermediate resonances are

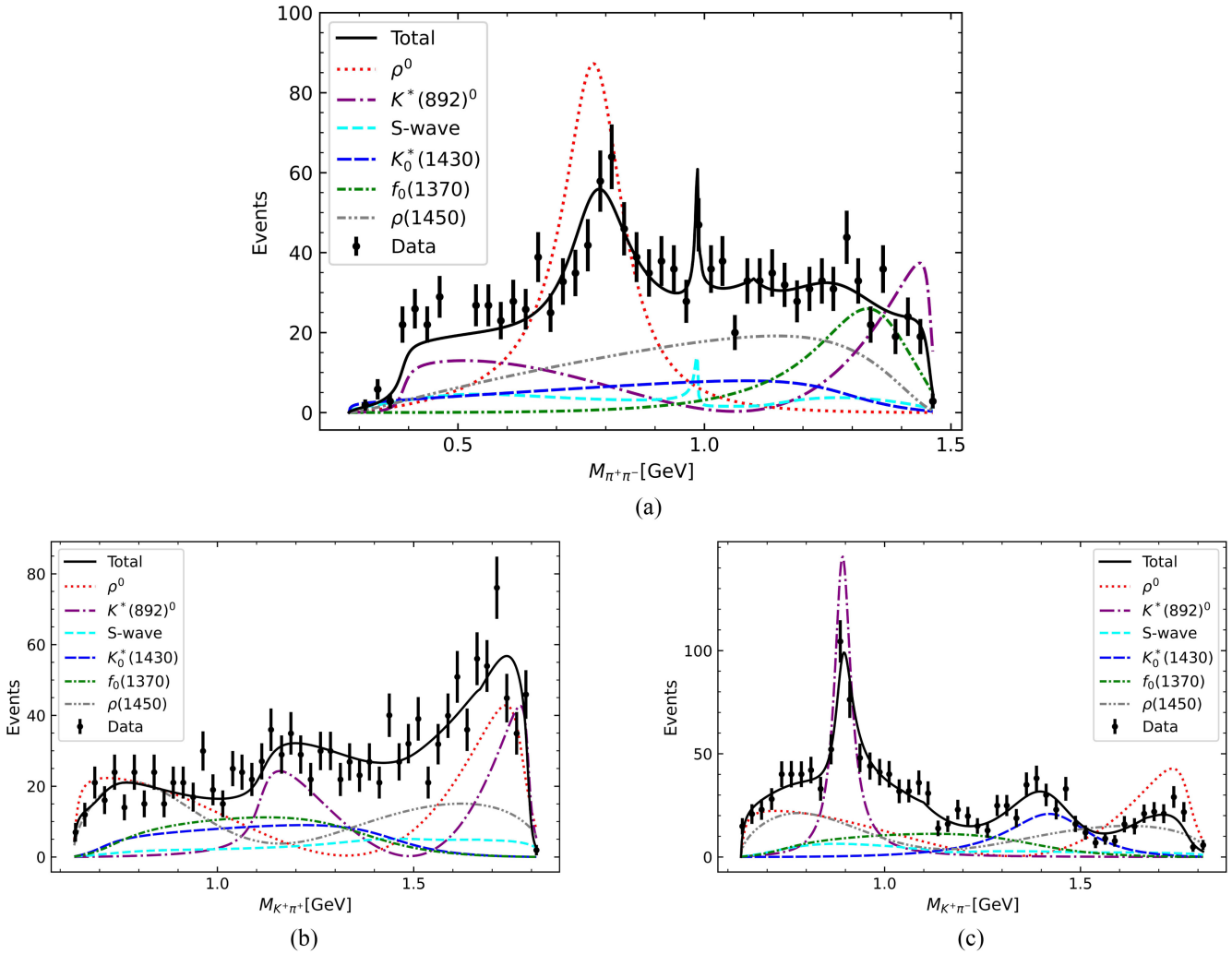

FIG. 5. Combined fit for the invariant mass distribution of the decay $D_s^+ \to \pi^+\pi^-K^+$: (a) $\pi^+\pi^-$, (b) $K^+\pi^+$, (c) $K^+\pi^-$. The solid (black) line is the total contributions of the S and P waves, the dashed (cyan) line represents the S-wave contribution, the dotted (red) line is the contribution of the ρ. The long-dash-dotted (purple), long-dashed (blue), dash-dotted (green), and dash-dot-dotted (gray) lines are the contributions of the $K^*(892)$, $K_0^*(1430)$, $f_0(1370)$, and $\rho(1450)$, respectively. The dot (black) points are the experimental data measured by the BESII Collaboration [17].

TABLE II. Branching fractions for various intermediate processes decaying into the final state $\pi^+\pi^-K^+$, compared with the results of the BESIII Collaboration [17] and PDG [30]. In our results, the first uncertainties are estimated from the experimental error of $B[D_S^+ \to K^*(892)^0\pi^+, K^*(892)^0 \to K^+\pi^-]$, and the second ones are from Eq. (35).

Decay process	Ours (10^{-3})	BESIII (10^{-3})	PDG (10^{-3})
$D_s^+ \to K^+ f_0(500)$	$0.38 \pm 0.03^{+0.03}_{-0.03}$	$0.43 \pm 0.14 \pm 0.24$	...
$D_s^+ \to K^+ f_0(980)$	$0.11 \pm 0.01^{+0.04}_{-0.04}$	$0.27 \pm 0.08 \pm 0.07$	...
$D_s^+ \to K^+\rho^0$	$2.94 \pm 0.27^{+0.03}_{-0.05}$	$1.99 \pm 0.20 \pm 0.22$	2.5 ± 0.4
$D_s^+ \to K^+ f_0(1370)$	$1.07 \pm 0.10^{+0.11}_{-0.20}$	$1.22 \pm 0.19 \pm 0.18$	...
$D_s^+ \to K_0^*(1430)^0\pi^+$	$1.06 \pm 0.10^{+0.01}_{-0.02}$	$1.15 \pm 0.16 \pm 0.15$	0.50 ± 0.35
$D_s^+ \to K^+\rho(1450)^0$	$2.38 \pm 0.22^{+0.04}_{-0.09}$	$0.78 \pm 0.20 \pm 0.17$	0.69 ± 0.64

almost consistent with the results obtained by the BESIII Collaboration in Ref. [17] and PDG [30] within the uncertainties.

IV. SUMMARY

Motivated by the BESIII Collaboration measurements for the decay $D_s^+ \to \pi^+\pi^-K^+$, we investigate this decay process by considering the final state interactions from the S-wave pseudoscalar-pseudoscalar interactions with the chiral unitary approach, where the resonances $f_0(500)$ and $f_0(980)$ are dynamically generated in the coupled channel interactions. In addition, we also take into account the contributions of the intermediate resonances $K^*(892)$, $K^*(1430)$, ρ, $\rho(1450)$, and $f_0(1370)$ (most of them in the P wave), which play a key role in the $D_s^+ \to \pi^+\pi^-K^+$ decay process. Considering the coherent effects between the S and P waves, one obtains the free parameters by fitting the experimental data and then can figure out the contributions of the S- and P-wave intermediate resonances. The obtained results show that the combined fit for the $\pi^+\pi^-$, $K^+\pi^+$, and $K^+\pi^-$ invariant mass distributions is consistent with experiments. However, the contributions of ρ and $\rho(1450)$ in the coherent fit is significantly bigger than experiments; also see their obtained branching fractions. Note that the peak around 0.98 GeV in the $\pi^+\pi^-$ mass distribution implies the signal of the $f_0(980)$, which is similar to the $\bar{B}^0 \to \pi^+\pi^-D^0$ decay. Meanwhile, we also calculate the branching fractions of the dominant decay channels, and it is obvious that the theoretical results are almost in agreement with the experimental measurements and PDG within the uncertainties, except for the branching ratios decaying into the intermediate resonances ρ and $\rho(1450)$ are a bit large and the one for the $f_0(980)$ becomes small.

Note added. Recently, the decay $D_s^+ \to K^+\pi^+\pi^-$ was also studied in Ref. [74] with similar formalism. In the present work, our fits for the data are improved by introducing the interference phases and more results for the branching fractions are presented.

ACKNOWLEDGMENTS

This work is supported by the Fundamental Research Funds for the Central Universities of Central South University under Grants No. 1053320214315 and No. 2022ZZTS0169, the Postgraduate Scientific Research Innovation Project of Hunan Province under Grant No. CX20220255, partly by the Natural Science Foundation of Changsha under Grant No. kq2208257, the Natural Science Foundation of Hunan province under Grant No. 2023JJ30647, and the National Natural Science Foundation of China under Grant No. 12365019.

[1] A. Ryd and A. A. Petrov, Rev. Mod. Phys. **84**, 65 (2012).
[2] Z. Lu (BESIII Collaboration), arXiv:2207.13397.
[3] P. L. Frabetti *et al.* (E687 Collaboration), Phys. Lett. B **351**, 591 (1995).
[4] R. E. Mitchell *et al.* (CLEO Collaboration), Phys. Rev. D **79**, 072008 (2009).
[5] P. del Amo Sanchez *et al.* (*BABAR* Collaboration), Phys. Rev. D **83**, 052001 (2011).
[6] J. P. Alexander *et al.* (CLEO Collaboration), Phys. Rev. Lett. **100**, 161804 (2008).
[7] P. del Amo Sanchez *et al.* (*BABAR* Collaboration), Phys. Rev. D **82**, 091103 (2010); **91**, 019901(E) (2015).
[8] A. Zupanc *et al.* (Belle Collaboration), J. High Energy Phys. 09 (2013) 139.
[9] P. U. E. Onyisi *et al.* (CLEO Collaboration), Phys. Rev. D **88**, 032009 (2013).

[10] M. Ablikim *et al.* (BESIII Collaboration), Phys. Rev. D **104**, 012016 (2021).
[11] B. Aubert *et al.* (*BABAR* Collaboration), Phys. Rev. D **79**, 032003 (2009).
[12] M. Ablikim *et al.* (BESIII Collaboration), Phys. Rev. D **106**, 112006 (2022).
[13] LHCb Collaboration, J. High Energy Phys. 07 (2023) 204.
[14] M. Ablikim *et al.* (BESIII Collaboration), Phys. Rev. Lett. **123**, 112001 (2019).
[15] M. Ablikim *et al.* (BESIII Collaboration), Phys. Rev. D **105**, L051103 (2022).
[16] M. Ablikim *et al.* (BESIII Collaboration), Phys. Rev. Lett. **129**, 182001 (2022).
[17] M. Ablikim *et al.* (BESIII Collaboration), J. High Energy Phys. 08 (2022) 196.
[18] J. M. Link *et al.* (FOCUS Collaboration), Phys. Lett. B **601**, 10 (2004).
[19] L. L. Chau, Phys. Rep. **95**, 1 (1983).
[20] W. I. Eshraim, F. Giacosa, and D. H. Rischke, Eur. Phys. J. A **51**, 112 (2015).
[21] J. Y. Wang, M. Y. Duan, G. Y. Wang, D. M. Li, L. J. Liu, and E. Wang, Phys. Lett. B **821**, 136617 (2021).
[22] J. A. Oller and E. Oset, Nucl. Phys. **A620**, 438 (1997); **A652**, 407(E) (1999).
[23] E. Oset and A. Ramos, Nucl. Phys. **A635**, 99 (1998).
[24] N. Kaiser, Eur. Phys. J. A **3**, 307 (1998).
[25] J. A. Oller, E. Oset, and J. R. Peláez, Phys. Rev. Lett. **80**, 3452 (1998).
[26] J. A. Oller and U.-G. Meißner, Phys. Lett. B **500**, 263 (2001).
[27] J. A. Oller, E. Oset, and A. Ramos, Prog. Part. Nucl. Phys. **45**, 157 (2000).
[28] J. M. Dias, F. S. Navarra, M. Nielsen, and E. Oset, Phys. Rev. D **94**, 096002 (2016).
[29] Z. Y. Wang, J. Y. Yi, Z. F. Sun, and C. W. Xiao, Phys. Rev. D **105**, 016025 (2022).
[30] R. L. Workman *et al.* (Particle Data Group), Prog. Theor. Exp. Phys. **2022**, 083C01 (2022).
[31] R. Escribano, P. Masjuan, and P. Sanchez-Puertas, arXiv: 2302.03312.
[32] F. Niecknig and B. Kubis, J. High Energy Phys. 10 (2015) 142.
[33] F. Niecknig and B. Kubis, Phys. Lett. B **780**, 471 (2018).
[34] R. Molina, J. J. Xie, W. H. Liang, L. S. Geng, and E. Oset, Phys. Lett. B **803**, 135279 (2020).
[35] Y. K. Hsiao, Y. Yu, and B. C. Ke, Eur. Phys. J. C **80**, 895 (2020).
[36] M. Y. Duan, J. Y. Wang, G. Y. Wang, E. Wang, and D. M. Li, Eur. Phys. J. C **80**, 1041 (2020).
[37] X. Z. Ling, M. Z. Liu, J. X. Lu, L. S. Geng, and J. J. Xie, Phys. Rev. D **103**, 116016 (2021).
[38] N. N. Achasov and G. N. Shestakov, Phys. Rev. D **107**, 056009 (2023).
[39] M. Ablikim *et al.* (BESIII Collaboration), J. High Energy Phys. 01 (2022) 052.
[40] H. Y. Cheng, C. W. Chiang, and Z. Q. Zhang, Phys. Rev. D **105**, 033006 (2022).
[41] H. Zhang, Y. H. Lyu, L. J. Liu, and E. Wang, Chin. Phys. C **47**, 043101 (2023).
[42] X. Luo, A. Xu, R. Li, and H. Sun, Phys. Rev. D **107**, 034035 (2023).
[43] X. Zhu, D. M. Li, E. Wang, L. S. Geng, and J. J. Xie, Phys. Rev. D **105**, 116010 (2022).
[44] L. R. Dai, E. Oset, and L. S. Geng, Eur. Phys. J. C **82**, 225 (2022).
[45] X. Zhu, H. N. Wang, D. M. Li, E. Wang, L. S. Geng, and J. J. Xie, Phys. Rev. D **107**, 034001 (2023).
[46] Z. Y. Wang, Y. W. Peng, J. Y. Yi, W. C. Luo, and C. W. Xiao, Phys. Rev. D **107**, 116018 (2023).
[47] N. N. Achasov, J. V. Bennett, A. V. Kiselev, E. A. Kozyrev, and G. N. Shestakov, Phys. Rev. D **103**, 014010 (2021).
[48] M. Ablikim *et al.* (BESIII Collaboration), Phys. Rev. D **92**, 052003 (2015); **93**, 039906(E) (2016).
[49] L. L. Chau and H. Y. Cheng, Phys. Rev. D **36**, 137 (1987).
[50] R. J. Morrison and M. S. Witherell, Annu. Rev. Nucl. Part. Sci. **39**, 183 (1989).
[51] L. Roca and E. Oset, Phys. Rev. D **103**, 034020 (2021).
[52] H. A. Ahmed, Z. Y. Wang, Z. F. Sun, and C. W. Xiao, Eur. Phys. J. C **81**, 695 (2021).
[53] Z. Wang, Y. Y. Wang, E. Wang, D. M. Li, and J. J. Xie, Eur. Phys. J. C **80**, 842 (2020).
[54] L. R. Dai, G. Y. Wang, X. Chen, E. Wang, E. Oset, and D. M. Li, Eur. Phys. J. A **55**, 36 (2019).
[55] G. Toledo, N. Ikeno, and E. Oset, Eur. Phys. J. C **81**, 268 (2021).
[56] J. Gasser and H. Leutwyler, Nucl. Phys. **B250**, 465 (1985).
[57] W. H. Liang and E. Oset, Phys. Lett. B **737**, 70 (2014).
[58] X. K. Guo, Z. H. Guo, J. A. Oller, and J. J. Sanz-Cillero, J. High Energy Phys. 06 (2015) 175.
[59] W. H. Liang, J. J. Xie, and E. Oset, Eur. Phys. J. C **75**, 609 (2015).
[60] G. Montaña, A. Ramos, L. Tolos, and J. M. Torres-Rincon, Phys. Rev. D **107**, 054014 (2023).
[61] J. A. Oller and E. Oset, Phys. Rev. D **60**, 074023 (1999).
[62] D. Gamermann, E. Oset, D. Strottman, and M. J. Vicente Vacas, Phys. Rev. D **76**, 074016 (2007).
[63] L. Alvarez-Ruso, J. A. Oller, and J. M. Alarcon, Phys. Rev. D **82**, 094028 (2010).
[64] Z. H. Guo, L. Liu, U.-G. Meißner, J. A. Oller, and A. Rusetsky, Phys. Rev. D **95**, 054004 (2017).
[65] C. Garcia-Recio, L. S. Geng, J. Nieves, and L. L. Salcedo, Phys. Rev. D **83**, 016007 (2011).
[66] A. Ozpineci, C. W. Xiao, and E. Oset, Phys. Rev. D **88**, 034018 (2013).
[67] Z. H. Guo, L. Liu, U.-G. Meißner, J. A. Oller, and A. Rusetsky, Eur. Phys. J. C **79**, 13 (2019).
[68] C. W. Xiao, J. X. Lu, J. J. Wu, and L. S. Geng, Phys. Rev. D **102**, 056018 (2020).
[69] Z. Y. Wang, H. A. Ahmed, and C. W. Xiao, Phys. Rev. D **105**, 016030 (2022).
[70] V. R. Debastiani, W. H. Liang, J. J. Xie, and E. Oset, Phys. Lett. B **766**, 59 (2017).
[71] J. A. Oller, E. Oset, and J. R. Peláez, Phys. Rev. D **59**, 074001 (1999); **60**, 099906(E) (1999); **75**, 099903(E) (2007).
[72] C. W. Xiao, U.-G. Meißner, and J. A. Oller, Eur. Phys. J. A **56**, 23 (2020).
[73] H. A. Ahmed and C. W. Xiao, Eur. Phys. J. A **59**, 245 (2023).
[74] L. R. Dai and E. Oset, arXiv:2307.03014.